Time-Varying Flexible Least Squares for Thermal Desorption of Gases

DAVID J. MIRON,[1] SHANE M. KENDELL,[2] ALAA M. MUNSHI,[1] ABDULLAH K. ALANAZI,[1] TREVOR C. BROWN[1]

[1]*School of Science and Technology, University of New England, Armidale,* NSW, 2351, *Australia*

[2]*Department of Chemistry, School of Science and Mathematics, Howard Payne University, Brownwood,* TX 76801

Received 19 August 2012; revised 22 October 2012; accepted 13 November 2012

DOI 10.1002/kin.20772
Published online 23 April 2013 in Wiley Online Library (wileyonlinelibrary.com).

ABSTRACT: Time-varying linear regression via flexible least squares is used to determine temperature-dependent kinetic parameters during low-pressure, steady-state, temperature-programmed desorption from catalytic surfaces. The flexible least squares approach optimizes time-varying parameters by minimizing dynamic and measurement discrepancies between a linear theoretical model and experimental data using linear regression. The effectiveness of this approach is demonstrated by calculation of accurate temperature-dependent activation energies, preexponential factors, and differential conversion functions for the evolution of 3-methyl-2-oxetanone (β-lactone) during the selective oxidation of isobutane over aluminum phosphomolybdates. © 2013 Wiley Periodicals, Inc. Int J Chem Kinet 45: 374–386, 2013

INTRODUCTION

Flexible least squares for time-varying linear regression (FLS-TVLR) for processes where modeled parameters evolve slowly and smoothly over time was first proposed by Kalaba and Tesfatsion in 1989 [1]. FLS-TVLR has subsequently been shown to be a powerful technique for temporal data mining to determine time-varying parameters, particularly for econometric processes [2–4]. The FLS-TVLR approach [1,2] assumes that, for any theoretical linear model proposed to explain observable data, there are two distinct types of discrepancy terms, *dynamic* and *measurement*. The *dynamic* terms account for time variation in successive parameter vectors, and the *measurement* terms account for differences between observed and theoretically predicted outcomes using linear regression. Optimization of the time-varying parameters is achieved by minimizing both the *dynamic* and the *measurement* residual squared errors.

The rates of evolution of gas-phase molecules from solid surfaces when the temperature is increased linearly with time are given by the Arrhenius expression

$$\beta \frac{\mathrm{d}\alpha}{\mathrm{d}T} = Af(\alpha) \exp\left(-\frac{E}{RT}\right) \tag{1}$$

where α is fraction of molecules evolved from the surface, T the temperature, β the linear heating rate ($\beta = \mathrm{d}T/\mathrm{d}t$), A the preexponential factor, E the activation energy, $f(\alpha)$ the differential function for fractional conversion, and R the gas constant. A differential function commonly used when all temperature-dependent

Correspondence to: Trevor Brown; e-mail: Trevor.Brown@une.edu.au.

Table I Rate Parameters Previously Determined for β-Lactone Evolution over $Al_{0.25}H_{2.25}[PMo_{12}O_{40}]$, $Al_{0.5}H_{1.5}[PMo_{12}O_{40}]$, and $Al[PMo_{12}O_{40}]$ Following Exposure to Isobutene [11]

	Gaussian Curve 1			Gaussian Curve 2		
Substrate	$\log_{10} A$	E (kJ mol^{-1})	Order, a	$\log_{10} A$	E (kJ mol^{-1})	Order, a
$Al_{0.25}H_{2.25}[PMo_{12}O_{40}]$	27.1 (2.0)	303 (22)	1.48 (0.11)	22.6 (1.7)	255 (19)	1.39 (0.10)
$Al_{0.5}H_{1.5}[PMo_{12}O_{40}]$	18.0 (1.1)	187 (12)	1.33 (0.08)	12.1 (0.3)	129 (4)	1.41 (0.04)
$Al[PMo_{12}O_{40}]$	17.2 (0.8)	176 (9)	1.41 (0.07)	13.5 (0.5)	138 (5)	1.38 (0.05)

Units for the preexponential factors include product abundance mass-spectral/molecular flow rate conversion factors (abundance^{-1} molecules s^{-1}). Associated errors are in parentheses.

rate data are available for an evolved gas is [5]

$$f(\alpha) = (1-\alpha)^a \tag{2}$$

where a is the order of the surface reaction. Many studies have been undertaken using a range of theoretical approaches to accurately measure activation energies, preexponential factors, and orders for thermal decomposition of solids [5,6], and for thermal desorption of gases [7,8]. It is clear from these studies that the temperature or conversion dependence of these parameters must be included in the analyses, due to lateral interactions between absorbed species [8], mass and heat transfer processes [5], surface heterogeneity and restructuring [9], and hence surface activation/deactivation. The complete and leading edge analyses methods have been shown to yield the most accurate coverage-dependence rate parameters for thermal desorption [7]. Compensation effects [8], isokinetic relationships [6], and invariant kinetic parameter (IKP) methods [10] can also impact on the analyses.

In this paper, temperature-dependent rate parameters are calculated using FLS-TVLR for the evolution of 3-methyl-2-oxetanone (β-lactone) during the selective oxidation of isobutane over $Al_{0.25}H_{2.25}[PMo_{12}O_{40}]$, $Al_{0.5}H_{1.5}[PMo_{12}O_{40}]$, and $Al[PMo_{12}O_{40}]$ [11]:

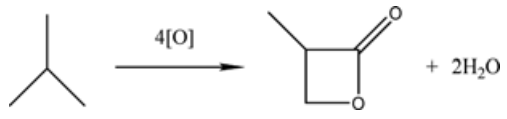

(3)

The β-lactone and water evolve following extraction of four oxygen atoms [O] from the surface of the aluminum phosphomolybdates.

Rate data have been obtained using low-pressure, steady-state, temperature-programmed reaction spectroscopy; a technique developed by this group [11–13]. Gas-phase species evolving from a solid substrate located in a low-pressure steady-state reactor are directly monitored by a quadrupole mass spectrometer. This technique minimizes secondary gas-phase reactions and heat fluctuations and allows for the collection of accurate rate data for the elementary steps to evolution from the solid surface.

The formation of β-lactone in the reaction of isobutane and phosphomolybdates has only been observed using this low-pressure technique [11]. A theoretical study using density function theory methods [14] has shown that the β-lactone is likely to be a precursor to the commercially important, methacrylic acid, which is a product *not* detected at low pressures. Methacrylic acid, however, is often observed as a product at higher pressures [15].

The β-lactone evolution data for the three substrates, analyzed in this paper, have previously been simulated using two Gaussian curves for each data set and then fitted with Arrhenius-type rate expressions to determine the rate parameters [11]. That is, the simulation assumes two surface reaction types leading to β-lactone desorption for each substrate. Table I lists the rate parameters obtained using this method. The resultant fit to the data is excellent, and reaction orders are equivalent for all six proposed surface reactions. However, magnitudes and trends in Arrhenius parameters are difficult to interpret.

EXPERIMENTAL TECHNIQUE AND DESORPTION DATA

Temperature-programmed reaction spectroscopy using a low-pressure steady-state technique has been developed by this group for the study of the kinetics of gas-solid reactions. Details of the technique, including sample preparation and characterization have been previously reported [11–13]. Briefly, the reactant gas (isobutane) mixed with argon flows continuously over a substrate ($Al_{0.25}H_{2.25}[PMo_{12}O_{40}]$, $Al_{0.5}H_{1.5}[PMo_{12}O_{40}]$, or $Al[PMo_{12}O_{40}]$) located in

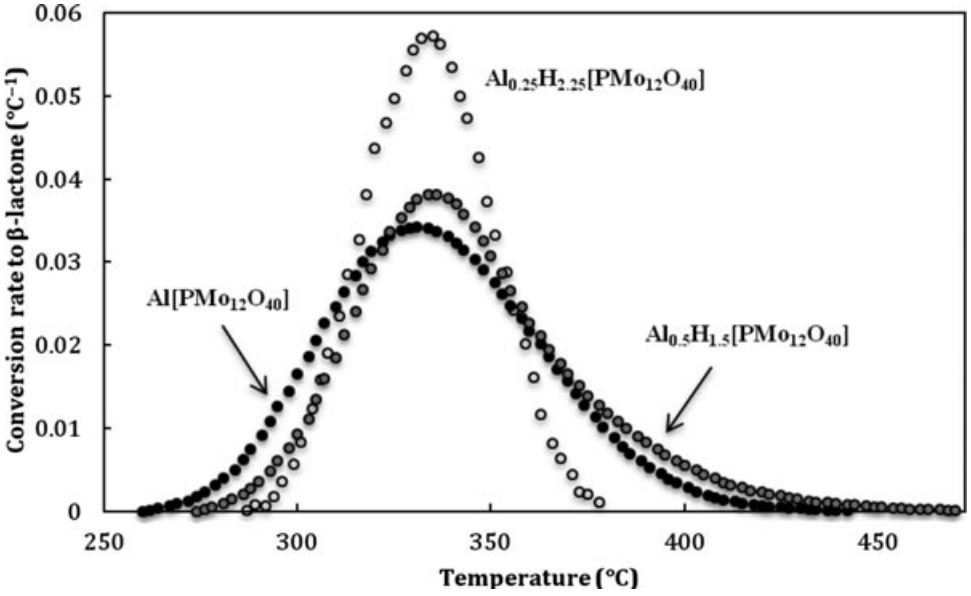

Figure 1 Evolution rates of β-lactone from the surfaces of the three substrates, $Al_{0.25}H_{2.25}[PMo_{12}O_{40}]$ (o), $Al_{0.5}H_{1.5}[PMo_{12}O_{40}]$ (•), or $Al[PMo_{12}O_{40}]$ (•) and from the Knudsen cell reactor.

a Knudsen cell reactor. Oxidation products, unreacted isobutane, and argon exit from the cell and pass directly into a quadrupole mass spectrometer (ionization voltage, 70 eV). Each sample was subjected to five temperature-programmed experiments (100–500°C at $\beta = 5$°C min^{-1}). For each experiment, isobutane flowed over the substrate for 2 h at 100°C, prior to commencing the heating. For all except the fifth experiment, the isobutane continued to flow over the substrate, during heating to 500°C. For the fifth experiment, the reactant flow was turned off and the system evacuated before commencing the temperature program. For all experiments, the resultant mass-spectral profiles consist of a range of evolved products—methacrolein, 3-methyl-2-oxetanone (β-lactone), acetic acid, carbon dioxide, and water. Evolution of β-lactone is characterized and hence monitored with mass spectral abundances, I_{68} at $m/e = 68$ ($C_4H_4O^+$), and the profiles as a function of temperature for each of the three substrates are shown in Fig. 1. Rates of conversion to β-lactone are calculated from

$$\frac{d\alpha_{68}}{dT} = \frac{I_{68,t}}{\sum_{t=0}^{T} I_{68,t}\,\Delta T} \tag{4}$$

where ΔT is the temperature difference between successive monitored abundances. These data taken from the fifth and hence desorption experiments, in the absence of flowing isobutane, for each substrate are used in this paper to demonstrate the effectiveness of the FLS-TVLR method.

Details of the aluminum phosphomolybdate syntheses have been previously reported, as have the physical characteristics listed in Table II [11]. Also in Table II are the temperature ranges over which the rates of β-lactone evolution have been simulated and parameters determined.

Table II Primitive Unit Cell Dimensions, BET (Brunauer, Emmett, Teller) Surface Areas, and Pore Volume for Each Substrate [11]

Substrate	Unit Cell Dimensions (Å)	BET Surface Area (m^2 g^{-1})	Pore Volume (cm^3 g^{-1})	T Range (°C)
$Al_{0.25}H_{2.25}[PMo_{12}O_{40}]$	13.399 (6)	1.82 (0.26)	13.399 (6)	287–378
$Al_{0.5}H_{1.5}[PMo_{12}O_{40}]$	13.391 (10)	1.21 (0.11)	13.391 (10)	274–470
$Al[PMo_{12}O_{40}]$	13.336 (7)	1.22 (0.12)	13.336 (7)	260–442

Associated errors are in parentheses. Temperature range refers to the range over which the β-lactone evolution rates have been optimized and parameters calculated.

Table III Ordinary Linear Least Squares Fitting for β-Lactone Evolution over $Al_{0.25}H_{2.25}[PMo_{12}O_{40}]$, $Al_{0.5}H_{1.5}[PMo_{12}O_{40}]$, and $Al[PMo_{12}O_{40}]$

Substrate	$\log_{10} A_{app}$ ($^{\circ}C^{-1}$)	E_{app} (kJ mol^{-1})	Order, a	R^2
$Al_{0.25}H_{2.25}[PMo_{12}O_{40}]$	24.6 (1.6)	300 (20)	1.37 (0.10)	0.871
$Al_{0.5}H_{1.5}[PMo_{12}O_{40}]$	12.9 (1.0)	169 (14)	1.62 (0.10)	0.808
$Al[PMo_{12}O_{40}]$	14.3 (0.7)	183 (10)	1.56 (0.07)	0.856

Associated errors are in parentheses.

RESULTS AND DISCUSSION

Data Analysis: Ordinary Linear Least Squares

The function often used to model rate data is the rate law:

$$\frac{d\alpha}{dT} = A_{app}(1-\alpha)^a \exp\left(-\frac{E_{app}}{RT}\right) \quad (5)$$

Taking natural logs

$$\ln\left(\frac{d\alpha}{dT}\right) = \ln\left(A_{app}\right) + a\ln(1-\alpha) - \frac{E_{app}}{RT} \quad (6)$$

leads to a linear equation with unknown parameters—the apparent Arrhenius preexponential factor $\ln\left(A_{app}\right)$, activation energy E_{app}, and reaction order a. Measurables are $d\alpha/dT$, $1-\alpha$, and T. Ordinary linear least squares are then employed to calculate the unknown parameters. These routine analyses were undertaken using the statistical computing language R [16], for three-parameter ($\ln A_{app}$, E_{app}, and a) simulations of the evolved β-lactone evolution rates from the three substrates. Optimized parameters are listed in Table III, and Fig. 2 demonstrates the goodness of fit for the rates of β-lactone formation over one of the substrates, $Al[PMo_{12}O_{40}]$.

The ordinary linear least square simulations to the data are not satisfactory, as evidenced by the poor coefficients of determination R^2 in Table III. Optimized rate parameters are similar in magnitude to the corresponding gas–solid reactions and parameters previously reported [11] and listed in Table I. For $Al_{0.5}H_{1.5}[PMo_{12}O_{40}]$ and $Al[PMo_{12}O_{40}]$ substrates, the magnitudes of the preexponential factors are larger than typical first-order molecular desorption factors (10^{13}–10^{16} s^{-1}) estimated using transition state theory [17]. This maybe due to the higher reaction orders of 1.37, 1.62, and 1.56, which are all reasonable and indicative of either combined first-order desorption and diffusion processes or involvement of the substrate in the β-lactone evolution. The large Arrhenius

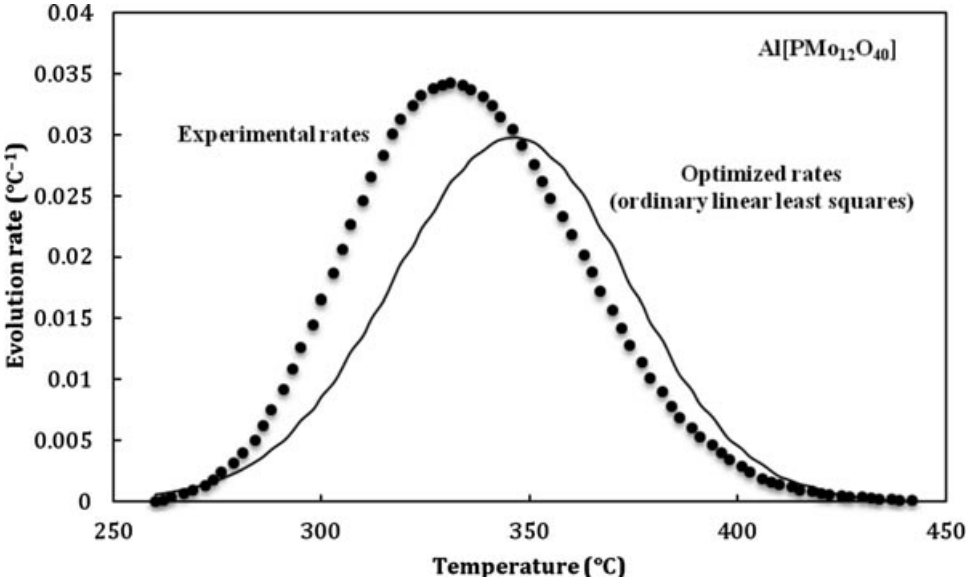

Figure 2 Experimental (•) and predicted (—) rates for β-lactone evolution from the surface of $Al[PMo_{12}O_{40}]$. Optimum rates are calculated from $d\alpha/dT = 10^{14.3}(1-\alpha)^{1.56}e^{-183/RT}$.

Table IV Three-parameter ($\log_{10}$ A_t, E_t, and a_t) FLS–TVLR Fitting for β-Lactone Evolution over $Al_{0.25}H_{2.25}[PMo_{12}O_{40}]$, $Al_{0.5}H_{1.5}[PMo_{12}O_{40}]$, and $Al[PMo_{12}O_{40}]$

Substrate	$\log_{10} A_t$ ($^\circ C^{-1}$)	E_t (kJ mol^{-1})	Order, a_t	Cost Function $C\left(b_{n,t};\mu, N, T\right)$
$Al_{0.25}H_{2.25}[PMo_{12}O_{40}]$	34.8–35.0	416.6–416.5	2.54–1.55	0.00242
$Al_{0.5}H_{1.5}[PMo_{12}O_{40}]$	35.4–35.7	422.1–421.9	5.04–2.67	0.00363
$Al[PMo_{12}O_{40}]$	33.2–33.5	393.0–392.8	4.89–2.40	0.00552

Cost functions (9) for each simulation are also listed.

parameters for $Al_{0.25}H_{2.25}[PMo_{12}O_{40}]$ are more difficult to rationalize.

Data Analysis: Flexible Least Squares for Time-Varying Linear Regression

Ordinary linear least squares provides a single set of parameters for each evolution rate curve, and so does not provide information on time-varying effects such as lateral interactions between absorbed species [8], mass and heat transfer processes [5], and surface heterogeneity and restructuring [9]. FLS–TVLR [1–3] is used to exactly simulate each data set by varying each of the parameters at each temperature. The resultant distribution provides accurate information on the heterogeneity of the gas-surface reactions.

FLS–TVLR is a generalization of ordinary linear regression by including time-variant regression parameters. For a series of observations $y_1, y_2, \ldots, y_T$ obtained at successive times 1, 2, $\ldots$, T, there are known predictor functions $h_1, h_2, \ldots, h_T$ that are dependent on N unknown parameters $b_{n,1}, b_{n,2}, \ldots, b_{n,T}$, which evolve slowly over time. These parameters are optimized by minimizing both an ordinary linear measurement specification,

$$y_t - h_t\left(b_{n,t}\right) \approx 0 \tag{7}$$

and a parameter dynamic specification,

$$b_{n,t+1} - b_{n,t} \approx 0 \tag{8}$$

The N time-dependent parameters are ultimately calculated by minimizing the following cost function:

$$C\left(b_{n,t};\mu, N, T\right) = \mu \sum_{n=1}^{N} \sum_{t=1}^{T-1} \left(b_{n,t+1} - b_{n,t}\right)^2 + \sum_{t=1}^{T} \left(y_t - h_t\left(b_{n,t}\right)\right)^2 \tag{9}$$

where μ is a weighting that minimizes the difference between subsequent parameters ($b_{n,t+1}$ and $b_{n,t}$). As μ approaches infinity, the parameter determination approaches the zero dynamic cost (ordinary least squares) solution [1,2]. When μ is set close to zero, priority is given to the dynamic specification and to estimates of the time-varying parameters [3] and hence a closer fit to the data. This effect was verified using the β-lactone desorption rate data, and for all FLS–TVLR calculations reported in this paper $\mu = 0.001$ was used.

For gas-solid rate data

$$y_t = \frac{d\alpha}{dT} \tag{10}$$

$$h_t\left(b_{n,t};\alpha, T\right) = A_t\left(1-\alpha\right)^{a_t} \exp\left(-E_t/RT\right) \tag{11}$$

$$b_{1,t} = \log_{10} A_t, b_{2,t} = a_t, b_{3,t} = E_t \tag{12}$$

and these temperature-dependent parameters are calculated using code provided by Kalaba and Tesfatsion [1] and adapted for the statistical computing language R [16]. FLS–TVLR simulations were undertaken for three-parameter ($\log_{10} A_t$, E_t, and a_t) fits to the evolved β-lactone evolution rates from the three substrates. Optimized temperature-dependent parameters are summarized in Table IV and plotted against conversion in Figs. 3–5.

The negligible cost functions listed in Table IV for the three simulations demonstrate the almost identical match to the measured evolution rates. Figure 3 shows that activation energy does not vary significantly (± 0.1 kJ mol^{-1}) across the full range of conversions for each of the three substrates. The ideal fit to the rate data is achieved by temperature-dependent variations to the preexponential factors (Fig. 4) and overall orders (Fig. 5). At low conversions to β-lactone, $\log_{10} A_t$ are ca. $10^{0.5-1.0}$ higher, then decline to steady-state values to complete conversion. Overall orders, a, decline markedly from highs of 2.54, 5.04, and 4.89 to lows of 1.55, 2.67, and 2.40 for $Al_{0.25}H_{2.25}[PMo_{12}O_{40}]$, $Al_{0.5}H_{1.5}[PMo_{12}O_{40}]$, and $Al[PMo_{12}O_{40}]$, respectively.

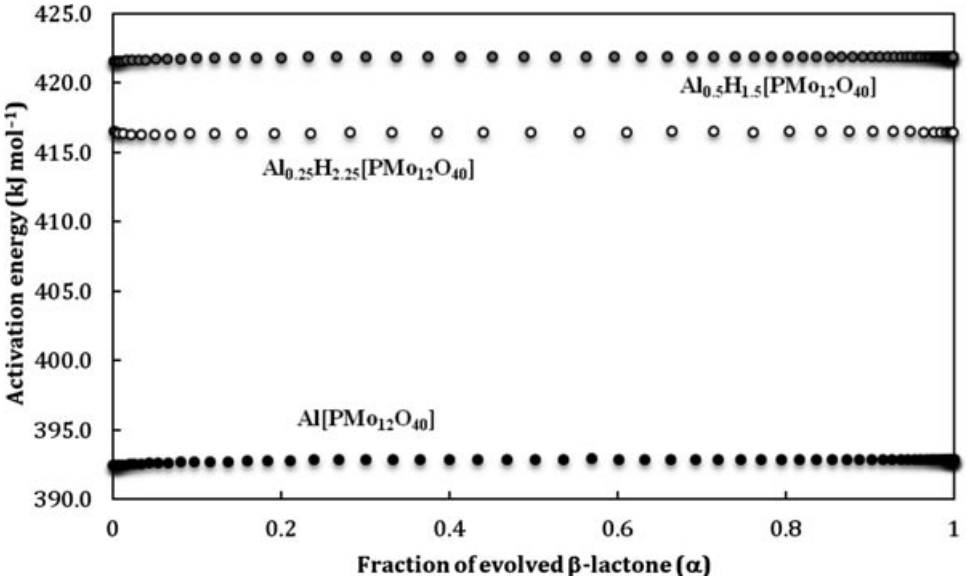

Figure 3 Temperature-varying activation energies as a function of conversion determined from FLS–TVLR fitting for β-lactone evolution from $Al_{0.25}H_{2.25}[PMo_{12}O_{40}]$ (o), $Al_{0.5}H_{1.5}[PMo_{12}O_{40}]$ (•), and $Al[PMo_{12}O_{40}]$ (•).

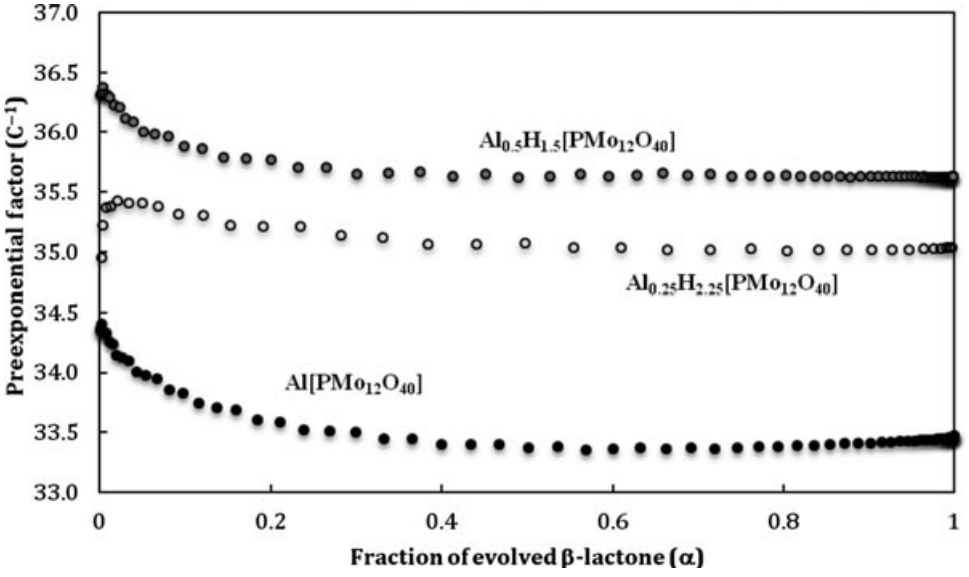

Figure 4 Temperature-varying preexponential factors as a function of conversion determined from FLS–TVLR fitting for β-lactone evolution from $Al_{0.25}H_{2.25}[PMo_{12}O_{40}]$ (o), $Al_{0.5}H_{1.5}[PMo_{12}O_{40}]$ (•), and $Al[PMo_{12}O_{40}]$ (•).

The magnitudes and trends in these parameters are difficult to explain in terms of the expected physical and chemical processes leading to β-lactone evolution. Large orders, a_t, seem unlikely to represent true orders of reaction, and so $f(\alpha) = (1-\alpha)^{a_t}$ is not the true differential function for fractional conversion [5]. Figure 6 shows plots of normalized $(1-\alpha)^{a_t}$ against fraction of evolved β-lactone for each of the three substrates, and plots are compared with the straight line when $a_t = 1.0$. The areas under each curve and straight line in Fig. 6 are the same to allow for comparisons between the substrates and functions. At low conversions, the fraction of β-lactone precursors available for the reaction is high and greater than unity. This may indicate that either there are excess precursors per active site for each substrate or other reactions (e.g., methacrolein formation) are competing for the same precursors. The similarity in the $Al_{0.5}H_{1.5}[PMo_{12}O_{40}]$

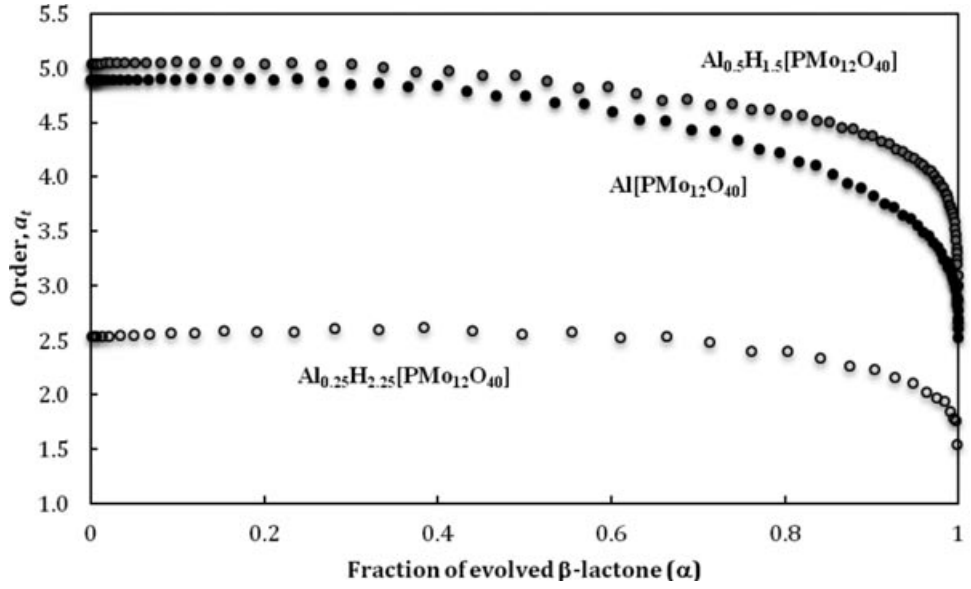

Figure 5 Temperature-varying overall orders as a function of conversion for β-lactone evolution from $Al_{0.25}H_{2.25}[PMo_{12}O_{40}]$ (o), $Al_{0.5}H_{1.5}[PMo_{12}O_{40}]$ (•), and $Al[PMo_{12}O_{40}]$ (•).

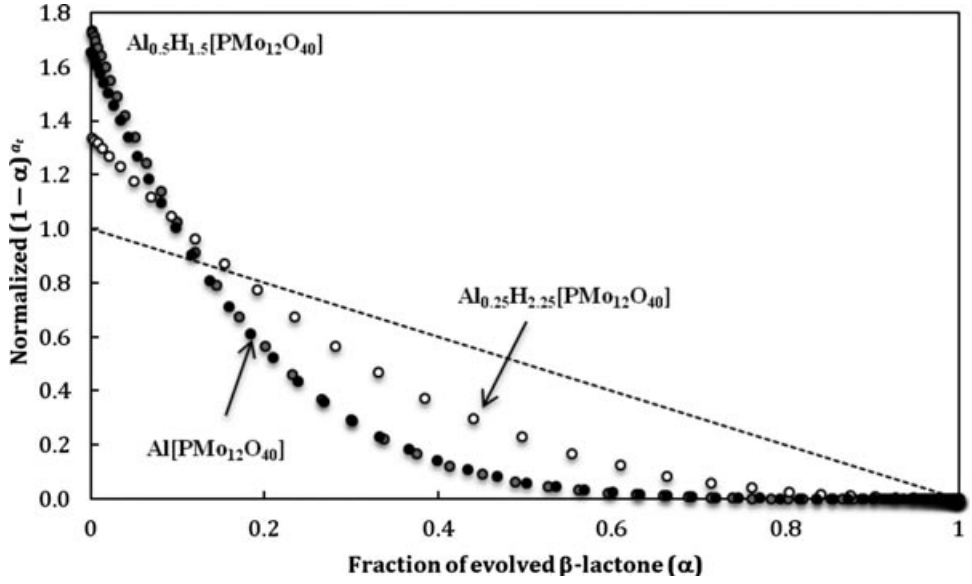

Figure 6 Apparent differential functions of conversion, $f(\alpha)$ from FLS–TVLR: temperature-varying normalized $(1-\alpha)^{a_t}$ as a function of conversion for β-lactone evolution from $Al_{0.25}H_{2.25}[PMo_{12}O_{40}]$ (o), $Al_{0.5}H_{1.5}[PMo_{12}O_{40}]$ (•), and $Al[PMo_{12}O_{40}]$ (•). The dashed straight line from $(1-\alpha)^{a_t} = 1.0$ to 0.0 is conversion when $a_t = 1.0$ for all three substrates.

and $Al[PMo_{12}O_{40}]$ differential functions in Fig. 6 suggests that $\log_{10} A_t$ and E_t should also be similar for these two substrates.

The very large preexponential factors cannot be explained by transition-state theory [17]. The very large activation energies are also anomalous, because they indicate that the fractions of molecules ($\exp(-E_t/RT)$), with enough energy to react are too small at these temperatures to observe any products. Conclusions on reactivity relative to aluminum or acid content or structure cannot be readily made from these parameters. While the optimized parameters represent the best fit to the data, the compensating relationship between the two Arrhenius parameters [8] leads to these distortions. In addition, this compensation impacts on the determination of the overall order and

Table V Two-Parameter ($\log_{10}$ A_t, E_t, and $a = 1.0, 1.5, 2.0$) FLS–TVLR Fitting for β-Lactone Evolution over $Al_{0.25}H_{2.25}[PMo_{12}O_{40}]$, $Al_{0.5}H_{1.5}[PMo_{12}O_{40}]$, and $Al[PMo_{12}O_{40}]$.

Substrate	$\log_{10} A_t$ ($^\circ C^{-1}$)	E_t (kJ mol^{-1})	Order, a	Cost Function $C\left(b_{n,t}; \mu, N, T\right)$
$Al_{0.25}H_{2.25}[PMo_{12}O_{40}]$	23.2–23.8	289.4–289.7	1.0	1.42
	32.1–32.7	389.0–389.3	1.5	1.67
	41.0–41.7	488.6–488.9	2.0	2.66
$Al_{0.5}H_{1.5}[PMo_{12}O_{40}]$	12.0–13.1	173.3–173.8	1.0	2.99
	17.6–18.7	235.6–236.1	1.5	3.09
	23.2–24.4	298.0–298.6	2.0	3.64
$Al[PMo_{12}O_{40}]$	13.5–14.6	186.6–187.2	1.0	3.68
	19.4–20.3	249.5–250.0	1.5	3.52
	25.1–26.2	312.3–312.9	2.0	3.83

Cost functions (9) for each simulation are also listed.

hence the true conversion function. That is, there are more than a single set of solutions using FLS-TVLR and a three-parameter fit, and for these data sets do not appear to provide realistic parameters.

Data Analysis: FLS-TVLR and Invariant Kinetic Parameters

The IKP method [10] is based on the observation that kinetic parameters ($\ln A$ and E) for a single data set (e.g., desorption rate profile) are linearly related when different models or conversion functions lead to different parameters for the same data set. This method is correlated with the compensation effect [8], where a linear relationship is also apparent for the kinetic parameters of equivalent activated complexes, but different reactants, intermediates or substrates. IKP (δ_1, δ_2) can be calculated from

$$\ln A = \delta_1 E + \delta_2 \tag{13}$$

This function can be substituted into the FLS-TVLR predictor function (11) to give

$$\ln\left(h_t\left(b_{n,t}; \alpha, T\right)\right) = \delta_2 + a_t \ln(1-\alpha) + \left(\delta_1 - \frac{1}{RT}\right) E_t \tag{14}$$

leading to a two-parameter fit to the data with

$$b_{1,t} = a_t, b_{2,t} = E_t \tag{15}$$

To calculate IKP δ_1, δ_2, FLS–TVLR simulations were undertaken for two-parameter ($\log_{10} A_t$, E_t and $a = 1.0, 1.5,$ and 2.0) fits to the evolved β-lactone evolution rates from $Al_{0.25}H_{2.25}[PMo_{12}O_{40}]$, $Al_{0.5}H_{1.5}[PMo_{12}O_{40}]$, and $Al[PMo_{12}O_{40}]$. Optimized temperature-dependent parameters are summarized in Table V.

Figure 7 is a plot of the average two-parameter FLS-TVLR modeled values ($a = 1.0, 1.5, 2.0$) for β-lactone desorption from the three substrates listed in Table V, and gives a straight line

$$\ln A = (0.2101 \pm 0.0018)\, E + (-6.28 \pm 0.55) \tag{16}$$

The FLS-TVLR predictor function (14) with IKP (16) is then

$$\ln\left(h_t\left(b_{n,t}; \alpha, T\right)\right) = -6.28 + a_t \ln(1-\alpha) + \left(0.2101 - \frac{1}{RT}\right) E_t \tag{17}$$

FLS–TVLR simulations with IKP were undertaken for two-parameter (E_t and a_t) fits to the evolved β-lactone evolution rates from the three substrates. Optimized temperature-dependent parameters are summarized in Table VI and plotted against conversion in Figs. 8 and 9. Figure 10 demonstrates the fit for the rates of β-lactone formation over $Al[PMo_{12}O_{40}]$. Temperature-dependent $\log_{10} A_t$ also listed in Table VI are calculated from E_t using IKP.

The goodness of fit shown in Fig. 10 and the small cost functions, relative to ordinary linear least square residuals (9.80, 42.4, and 30.9 for $Al_{0.25}H_{2.25}[PMo_{12}O_{40}]$, $Al_{0.5}H_{1.5}[PMo_{12}O_{40}]$, and $Al[PMo_{12}O_{40}]$, respectively) listed in Table VI, demonstrate that the temperature-dependent parameters provide an excellent match to the rate data. Small variations between the simulated and experimental rates at low temperatures correspond to large fluctuations in the parameters at low conversions (Figs. 8 and 9). After this initial period, the preexponential factors and activation energies stabilize to constant values for each substrate. These steady-state values are shown

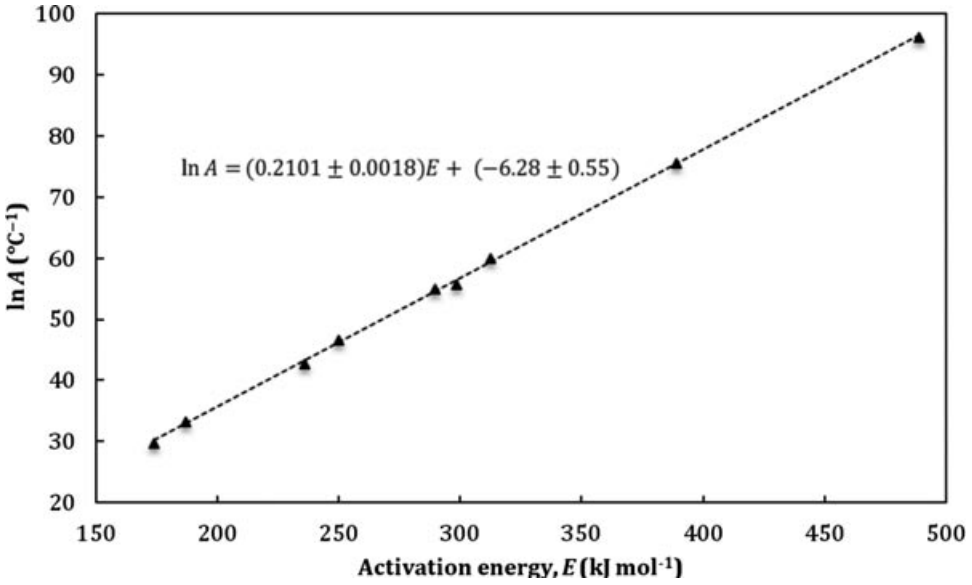

Figure 7 Plot of the average ln A ($2.303 \times \log_{10} A$) and E listed in Table V for two-parameter ($a = 1.0$, 1.5 and 2.0) FLS-TVLR fitting of β-lactone evolution rates from $Al_{0.25}H_{2.25}[PMo_{12}O_{40}]$, $Al_{0.5}H_{1.5}[PMo_{12}O_{40}]$, and $Al[PMo_{12}O_{40}]$. The dashed line is the line of best fit.

Table VI Two-Parameter (a_t and E_t) FLS–TVLR Using IKP Fitting for β-Lactone Evolution over $Al_{0.25}H_{2.25}[PMo_{12}O_{40}]$, $Al_{0.5}H_{1.5}[PMo_{12}O_{40}]$, and $Al[PMo_{12}O_{40}]$

Substrate	$\log_{10} A_t$ ($^\circ C^{-1}$)	E_t (kJ mol^{-1})	Order, a_t	Cost Function $C\left(b_{n,t}; \mu, N, T\right)$
$Al_{0.25}H_{2.25}[PMo_{12}O_{40}]$	27.7–**26.7**	333.6–**323.0**	–70.0 to **1.15**	1.90
$Al_{0.5}H_{1.5}[PMo_{12}O_{40}]$	19.6–**13.7**	245.2–**179.5**	–108 to **1.25**	5.81
$Al[PMo_{12}O_{40}]$	16.4–**5.71**	210.1–**92.5**	–109 to **0.74**	7.45

Temperature-dependent $\log_{10} A_t$ is calculated from E_t using Eq. (16). In bold are steady-state parameters observed for the majority of the conversion. Cost functions (9) for each simulation are also listed.

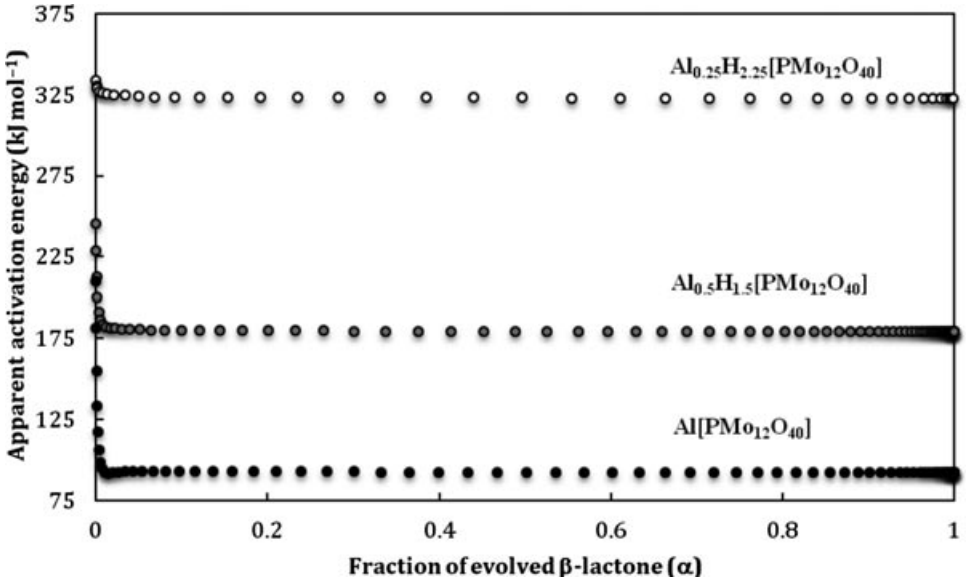

Figure 8 Temperature-varying activation energies as a function of conversion determined from FLS–TVLR using IKP fitting for β-lactone evolution from $Al_{0.25}H_{2.25}[PMo_{12}O_{40}]$ (o), $Al_{0.5}H_{1.5}[PMo_{12}O_{40}]$ (•), and $Al[PMo_{12}O_{40}]$ (•).

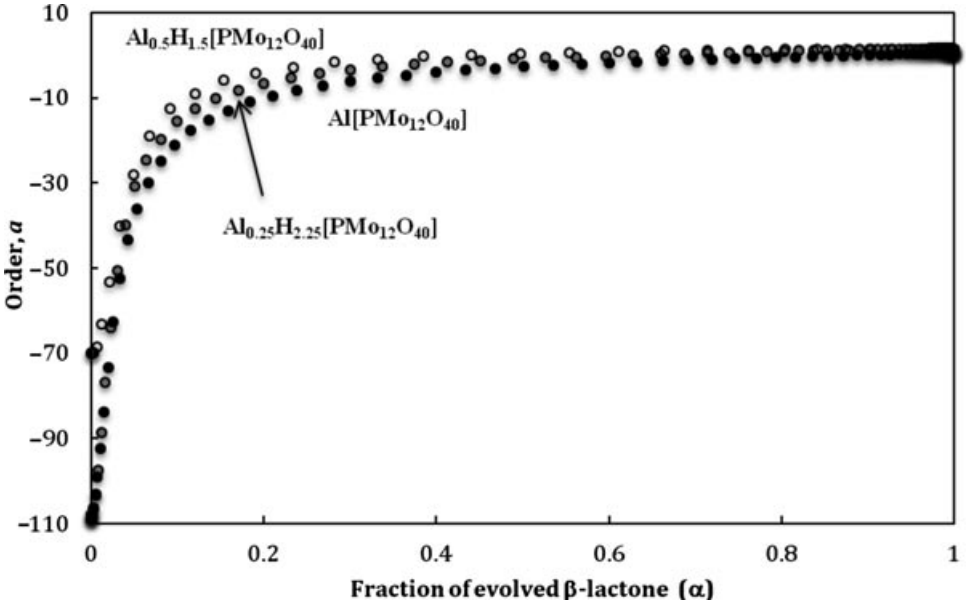

Figure 9 Temperature-varying overall orders as a function of conversion determined from FLS–TVLR using IKP fitting for β-lactone evolution from $Al_{0.25}H_{2.25}[PMo_{12}O_{40}]$ (o), $Al_{0.5}H_{1.5}[PMo_{12}O_{40}]$ (•), and $Al[PMo_{12}O_{40}]$ (•).

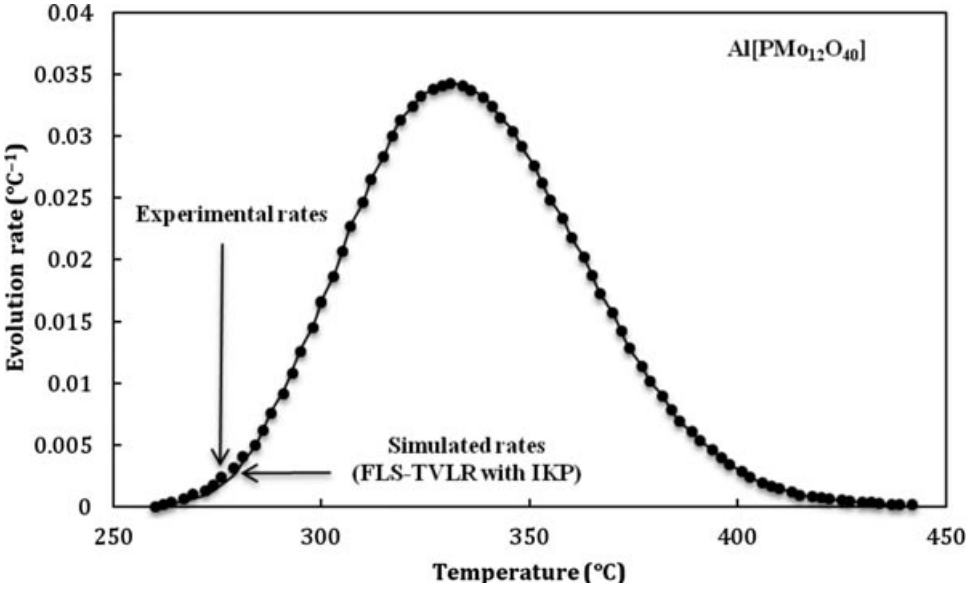

Figure 10 Experimental (•) and predicted (—) rates for β-lactone evolution from the surface of $Al[PMo_{12}O_{40}]$. Optimum rates are calculated from the FLS-TVLR with IKP temperature-dependent parameters listed in Table VI.

in bold in Table VI. The order, a_t, increases throughout the temperature range and becomes positive only at conversions greater than 90%.

Large and negative orders again seem unlikely to represent true orders of reaction, and so $f(\alpha) = (1-\alpha)^{a_t}$ are not the true differential functions for fractional conversion [5]. Figure 11 presents plots of normalized $(1-\alpha)^{a_t}$ against fraction of evolved β-lactone for each of the three substrates. For each substrate, the differential function rises to a maximum at $\alpha = 0.05$, 0.08, and 0.2 for $Al_{0.25}H_{2.25}[PMo_{12}O_{40}]$, $Al_{0.5}H_{1.5}[PMo_{12}O_{40}]$, and $Al[PMo_{12}O_{40}]$, respectively, and followed by an exponential decline. The shapes of the functions in Fig. 11 demonstrate the heterogeneity of the desorption process and are consistent with surface or bulk diffusion of the evolved β-lactone

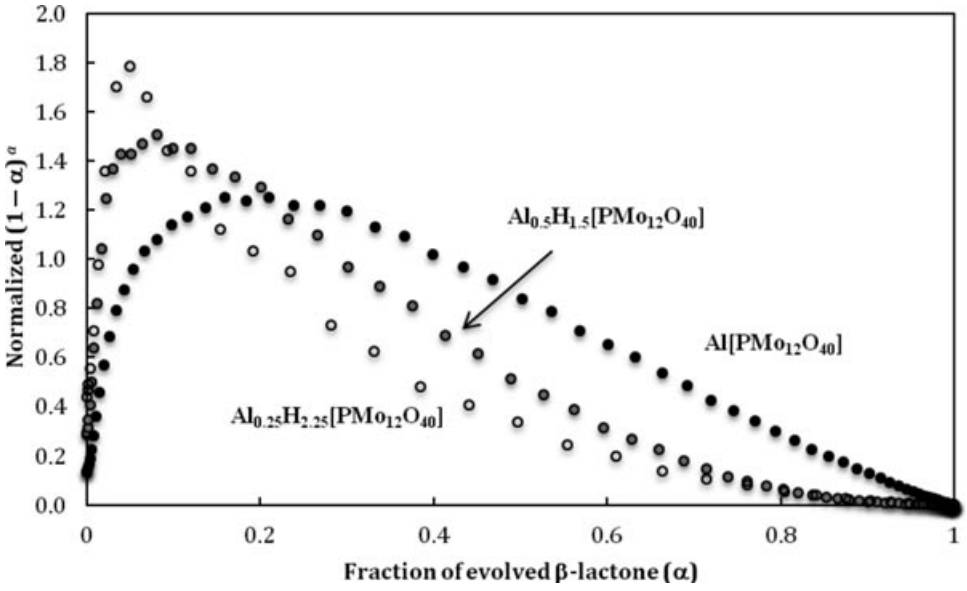

Figure 11 Apparent differential functions of conversion, $f(\alpha)$ from FLS–TVLR using IKP: temperature-varying normalized $(1-\alpha)^{a_t}$ as a function of conversion for β-lactone evolution from $Al_{0.25}H_{2.25}[PMo_{12}O_{40}]$ (o), $Al_{0.5}H_{1.5}[PMo_{12}O_{40}]$ (•), and $Al[PMo_{12}O_{40}]$ (•).

precursor initially dominating the rate. This is then followed by the reaction followed by desorption at higher conversions. It follows that the broader distribution for $Al[PMo_{12}O_{40}]$ is indicative of substantial diffusion limitations throughout the evolution. The associated maxima, or fraction of available β-lactone precursors are greater than unity in each case for a significant fraction of the desorption temperature range. This can be a consequence of either the precursors to β-lactone desorption per active site being greater than one or other reactions (e.g., methacrolein formation) are competing for the same precursors.

The very large $\log_{10} A$ for $Al_{0.25}H_{2.25}[PMo_{12}O_{40}]$ and small magnitude for $Al[PMo_{12}O_{40}]$ cannot be readily explained by transition-state theory [17], and the very large activation energies for $Al_{0.25}H_{2.25}[PMo_{12}O_{40}]$ indicate that the fraction of molecules ($\exp(-E_t/RT)$), with enough energy to react is too small at these temperatures for observable products. The Arrhenius parameters for $Al_{0.5}H_{1.5}[PMo_{12}O_{40}]$ are appropriate. Realistic parameters can be achieved if it is assumed that the active sites facilitating desorption are $2 \times Al_{0.25}H_{2.25}[PMo_{12}O_{40}]$, $1 \times Al_{0.5}H_{1.5}[PMo_{12}O_{40}]$, and $0.5 \times Al[PMo_{12}O_{40}]$, and the parameters adjusted to achieve the same rate. Therefore, the differential function becomes

$$\frac{d\alpha}{dT} = A f(\alpha)^b \exp\left(-\frac{E}{RT}\right) \tag{18}$$

where $b = 2$, 1, or 0.5, depending on $Al_{0.5}$ density within each substrate. The preexponential factors are then adjusted by $1/b$:

$$\ln\left(\frac{d\alpha}{dT}\right) = \left(\frac{1}{b}\right) \ln A_t + b \ln f(\alpha) - \frac{E_t}{RT} \tag{19}$$

Activation energies are subsequently calculated using IKP (16). Hence, steady-state rate coefficients, k, for β-lactone evolution are

$$k(Al_{0.25}H_{2.25}[PMo_{12}O_{40}]) = 10^{13.4\pm0.8^\circ} C^{-1} \exp\left(-176 \pm 7 \text{ kJ mol}^{-1}/RT\right) \tag{20}$$

$$k(Al_{0.5}H_{1.5}[PMo_{12}O_{40}]) = 10^{13.7\pm0.6^\circ} C^{-1} \exp\left(-180 \pm 5 \text{ kJ mol}^{-1}/RT\right) \tag{21}$$

$$k(Al[PMo_{12}O_{40}]) = 10^{11.4\pm0.6^\circ} C^{-1} \exp\left(-155 \pm 5 \text{ kJ mol}^{-1}/RT\right) \tag{22}$$

Errors are estimated from the errors in the IKP, as well as errors in the experimental procedure (substrate synthesis and technique).

Units for the preexponential factors can be converted to s^{-1} by multiplying by the heating rate (5°C min^{-1} or 0.083°C s^{-1}). Resultant magnitudes are $10^{10.3}$, $10^{12.6}$, and $10^{12.3}$ s^{-1}, respectively. These preexponential factors and activation energies (20)–(22) are equivalent for $Al_{0.25}H_{2.25}[PMo_{12}O_{40}]$ and $Al_{0.5}H_{1.5}[PMo_{12}O_{40}]$, whereas the activation energy is 23 ± 10 kJ mol^{-1} lower for $Al[PMo_{12}O_{40}]$. This last substrate has no intrinsic Brönsted acidity, and so the observed higher activity may indicate that H^+ retards the rate of β-lactone evolution, relative to the Al^{3+}. The role of H^+ in catalysis involving heteropolyanions has been reported to be as a charge carrier enhancing migration in the bulk of the substrate [11,18]. The preexponential factor, however, for the $Al[PMo_{12}O_{40}]$ is smaller than predicted by transition state theory for first-order desorption (10^{13}–10^{16} s^{-1}) [17]. An alternative explanation for the lower Arrhenius rate parameters is that both reaction and diffusion of isobutane and β-lactone precursors via the higher density of Al^{3+} cations are rate limiting. Diffusion coefficients generally have preexponential factors [19] that are lower than those calculated from transition state theory. The shapes of the differential functions of conversion in Fig. 11 concur with the conclusion that diffusion limitations are expected to be most significant for the $Al[PMo_{12}O_{40}]$, which has the broadest profile.

CONCLUSIONS

FLS-TVLR has been used to calculate the temperature-varying rate parameters for the evolution of β-lactone from three aluminum phosphomolybdate substrates ($Al_{0.25}H_{2.25}[PMo_{12}O_{40}]$, $Al_{0.5}H_{1.5}[PMo_{12}O_{40}]$, and $Al[PMo_{12}O_{40}]$), following exposure to isobutane. The modeled rate law is

$$\frac{d\alpha}{dT} = A_t\,(1-\alpha)^{a_t} \exp\left(\frac{E_t}{RT}\right) \tag{23}$$

and the temperature-dependent rate parameters are A_t, a_t, and E_t. This gave an almost perfect fit to the evolution rate data, with negligible variations in the activation energies across each temperature range and minor variations in the preexponential factors. The orders, a_t, however varied significantly; order at zero conversion was double the order at complete conversion, for each substrate. Magnitudes of each of the fitted parameters are difficult to interpret in terms of the chemical and physical processes leading to the β-lactone desorption.

By combining FLS-TVLR with IKP, only two temperature-varying rate parameters need to be calculated to model the evolution rate data. The modeled rate law becomes

$$\frac{d\alpha}{dT} = (1-\alpha)^{a_t} \exp\left(\delta_1 E_t + \delta_2 - \frac{E_t}{RT}\right) \tag{24}$$

where δ_1 and δ_2 are IKP relating the preexponential factors and activation energies. The calculated temperature-dependent rate parameters are a_t and E_t and also give an excellent fit to the data. Here the activation energies remain constant for almost all the conversion, whereas there are large changes and unrealistic magnitudes for the temperature-dependent orders. The heterogeneity of the desorption processes is apparent in these orders, and the implication is that the differential function of conversion $(1-\alpha)^{a_t}$ is not the true function. The actual functions are plotted in Fig. 11 and include both diffusion and reaction. Furthermore, the magnitudes of the Arrhenius parameters imply the rates are proportional to the density of $Al_{0.5}$ sites and 2.0, 1.0, and 0.5 are the actual orders for $Al_{0.25}H_{2.25}[PMo_{12}O_{40}]$, $Al_{0.5}H_{1.5}[PMo_{12}O_{40}]$, and $Al[PMo_{12}O_{40}]$, respectively. Furthermore, the corrected preexponential factors for $Al[PMo_{12}O_{40}]$ suggest surface or bulk diffusion limiting processes are occurring.

The combined FLS–TVLR with IKP method leading to rate coefficients (20)–(22), and differential functions of conversion plotted in Fig. 11 lead to the most accurate and effective simulations of the β-lactone evolution rate data.

BIBLIOGRAPHY

1. Kalaba, R.; Tesfatsion, L. Comput Math Appl 1989, 17(8/9), 1215–1245.
2. Kalaba, R.; Tesfatsion, L. Comput Stat Data Anal 1996, 21, 193–214.
3. Montana, G.; Triantafyllopoulos, K.; Tsagaris, T. Expert Syst Appl 2009, 36, 2819–2830.
4. Morana, C. Comput Stat 2009, 24, 459–479.
5. Budrugeac, P.; Segal, E. Int J Chem Kinet 2001, 33(10), 564–573.
6. Vyazovkin, S.; Linert, W. J Chem Inform Comp Sci 1994, 34, 1273–1278.
7. de Jong, A. M.; Niemantsverdriet, J. W. Surf Sci 1990, 233, 355–365.
8. Nieskens, D. L. S.; van Bavel, A. P.; Niemantsverdriet, J. W. Surf Sci 2003, 546, 159–169.
9. Zhdanov, V. P.; Kasemo, B. J Stat Phys 1998, 90(1/2), 79–101.

10. Lesnikovich, A. I.; Levchik, S. V. J Therm Anal 1983, 27, 89–94.
11. Kendell, S. M.; Alston, A.-S.; Ballam, N. J.; Brown, T. C.; Burns, R. C. Catal Lett 2011, 141, 374–390.
12. Le Minh, C.; Brown, T. C. Appl Catal A: Gen 2006, 310(7), 145–154.
13. Kendell, S. M.; Brown, T. C.; Burns, R. C. Catal Today 2008, 131, 526–532.
14. Nguyen, N. H.; Kendell, S. M.; Le Minh C.; Brown, T. C. Catal Lett 2010, 136, 28–34.
15. Cavani, F.; Mezzogori, R.; Pigamo, A.; Trifiro, F.; Etienne, E. Catal Today 2001, 71, 97–110.
16. R Core Team (2012). R: A Language and Environment for Statistical Computing. R Foundation for Statistical Computing: Vienna, Austria. Available at http://www.R-project.org/.
17. Mhadeshwar, A. B.; Wang, H.; Vlachos, D. G. J Phys Chem B 2003, 107, 12721–12733.
18. Mioc, U. B.; Petkovic, M.; Davidovic, M.; Peric, M.; Abdul-Redah, T. J Mol Struct 2008, 885, 131–138.
19. Aryafar, M.; Zaera, F. Catal Lett 1997, 48, 173–183.